ELSEVIER

Journal of Power Sources 74 (1998) 188–197

JOURNAL OF POWER SOURCES

The influence of some additives on the electrochemical behaviour of sintered nickel electrodes in alkaline electrolyte

Delia Maria Constantin, Eleonora Maria Rus *, L. Oniciu, Lucretia Ghergari

Department of Physical Chemistry, Faculty of Chemistry and Chemical Engineering of 'Babes-Bolyai' University, Arany Janos 11, 3400, Cluj-Napoca, Romania

Received 29 September 1997; accepted 19 January 1998

Abstract

Sintered nickel electrodes containing cobalt and cadmium hydroxides as additives were prepared by anodic polarization in 42 wt.% KOH solution of sintered nickel supports impregnated with mixed metal nitrate solutions. The structural and electrochemical characteristics of these electrodes were investigated by scanning electron microscopy, X-ray diffraction, cyclic voltammetry and charge–discharge curves. The addition of $Co(OH)_2$ and $Cd(OH)_2$ in active material have been shown to increase the discharge capacity and coulombic efficiency of nickel electrode by improvement of the electrode processes reversibility and by minimizing of the parasitic oxygen evolution reaction. © 1998 Elsevier Science S.A. All rights reserved.

Keywords: Sintered nickel electrodes; Alkaline electrolyte; Nickel hydroxide; Cobalt hydroxide; Cadmium hydroxide; Additives

1. Introduction

The nickel hydroxide electrode has been the object of many studies because of its utilization as cathode in alkaline batteries: nickel–cadmium, nickel–iron, nickel–zinc, nickel–hydrogen, and most recently, in nickel–metal hydride systems [1].

The active material of the nickel electrode consists of Ni(II) hydroxide, in discharged state and Ni(III) oxihydroxide in charged state. Two distinct couples, β-$Ni(OH)_2/\beta$-NiOOH and α-$Ni(OH)_2/\gamma$-NiOOH, can participate in the charge–discharge reactions of the nickel electrode [2,3].

The electrochemical characteristics and the performances of nickel electrode depend of structural forms of active material.

The transitions of these couples take place according to Bode (Eq. (1)) [4]:

$$\begin{tikzcd}
\beta\text{-Ni(OH)}_2 \arrow[r, "\text{ageing}"] \arrow[d, shift left, "-e^- \; -H^+"] & \alpha\text{-Ni(OH)}_2 \arrow[d, shift left, "-e^- \; -H^+"] \\
\beta\text{-NiOOH} \arrow[u, shift left, "+e^- \; +H^+"] \arrow[r, "\text{overcharge}"] & \gamma\text{-NiOOH} \arrow[u, shift left, "+e^- \; +H^+"]
\end{tikzcd} \quad .(1)$$

The discharge of the electrodes containing β-NiOOH proceeds at more positive potentials than that of the electrodes having γ-NiOOH. The discharge capacity is higher for electrodes containing γ-NiOOH due to a nickel oxidation state of 3.7–3.8, while for β-NiOOH, it only slightly exceeds 3 [5–8].

The charge process of nickel electrode occurs usually in competition with oxygen evolution expressed by Eq. (2):

$$4OH^- \rightarrow O_2\uparrow + 2H_2O + 4e^-. \qquad (2)$$

---

* Corresponding author.

0378-7753/98/$19.00

Table 1
The compositions of the mixed metal nitrate solutions

Electrode	Immersion solution			
	H_2O(l)	$Ni(NO_3)_2 \cdot 6H_2O$ (g)	$Co(NO_3)_2 \cdot 6H_2O$ (g)	$Cd(NO_3)_2 \cdot 4H_2O$ (g)
Ni + Co	0.3	540	59.82	–
Ni + Cd	0.3	540	–	40.18
Ni + Co + Cd	0.3	540	29.91	20.09

For an efficient charge of nickel cathode, the oxygen evolution must be minimized.

The addition of some metal hydroxides to the active material and lithium hydroxide to the electrolyte has a great influence on the electrochemical behaviour of the nickel electrode [6–13].

2. Experimental

Nickel electrodes were prepared by an electrochemical activation of the sintered nickel supports, realized from nickel powder obtained by thermolysis of $Ni(NO_3)_2 \cdot 6H_2O$ [14]. The sintered supports were immersed in a saturated solution of $Ni(NO_3)_2 \cdot 6H_2O$ for 24 h, at room temperature, and then were dried at 80°C for 2 h. After impregnation with the nickel nitrate, the supports were anodically polarized between two nickel plates (99.89 wt.% Ni) cathodes, in 42 wt.% KOH electrolyte, at a current density of 30 mA/cm^2 for an hour.

Electrodes containing inactive material cobalt and cadmium hydroxides as additives were prepared by the same method. Thus, the sintered nickel supports were immersed in mixed metal nitrate solutions before anodic polarization. The compositions of nitrate solutions are presented in the Table 1.

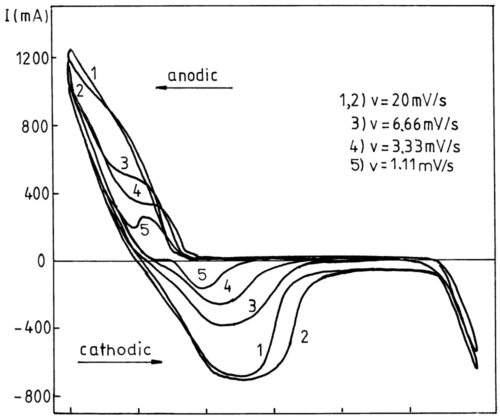

Fig. 1. Cyclic voltammograms of sintered nickel electrode in 6N KOH + 35 g/l LiOH, at $\upsilon = 20$ (1, 2), 6.66 (3), 3.33 (4), and 1.11 mV/s (5).

Binary electrodes, Ni + Co and Ni + Cd, consisting of nickel hydroxide with calculated contents of 10 wt.% $Co(OH)_2$, and 10 wt.% $Cd(OH)_2$, respectively, and a ternary electrode, Ni + Co + Cd, consisting of nickel hydroxide with 5 wt.% $Co(OH)_2$, and 5 wt.% $Cd(OH)_2$ were prepared. The amounts of additives ($Co(OH)_2$ and $Cd(OH)_2$) were only stoichiometric calculated on the basis of the precipitation reactions of that hydroxides from nitrates, considering 100% efficiencies and not experimentally determined.

The electrochemical behaviour of these electrodes has been investigated by cyclic voltammetry and charge–discharge curves.

The cyclic voltammetry measurements were made in a

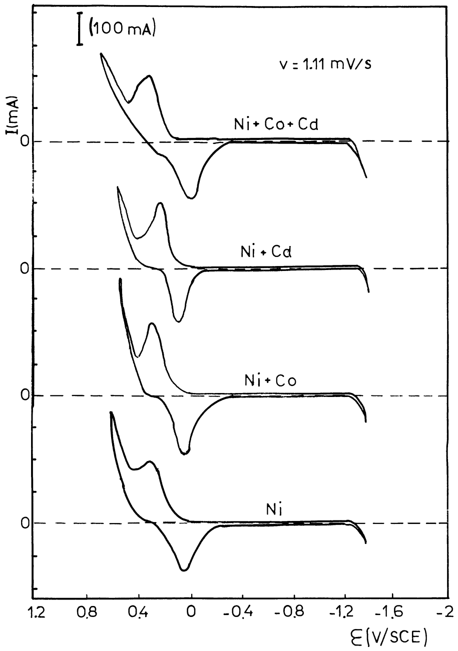

Fig. 2. Cyclic voltammograms of Ni, Ni + Co, Ni + Cd, and Ni + Co + Cd electrodes, in 6N KOH + 35 g/l LiOH, at $\upsilon = 1.11$ mV/s.

Table 2
Cyclic voltammetry measurements of sintered nickel electrodes at $v = 1.11$ mV/s, in 6N KOH + 35 g/l LiOH electrolyte

Electrode	$\varepsilon_{a,p}$ (V)	$\varepsilon_{c,p}$ (V)	$\Delta\varepsilon_p$ (V)	ε' (V)	$I_{c,p}/I_{a,p}$
Ni	0.340	0.085	0.255	0.212	0.89
Ni + Co	0.300	0.070	0.230	0.185	0.90
Ni + Cd	0.290	0.140	0.150	0.215	0.90
Ni + Co + Cd	0.300	0.075	0.225	0.188	0.91

conventional three-electrode cell using SCE as reference, connected through a Luggin capillary, and a platinum wire as counter electrode. All the potentials given in this paper are referred to SCE. The apparent surface area of the working electrode is 1 cm^2.

The electrolyte was 6N KOH solution containing 35 g/l LiOH as additive, because the favourable effect of LiOH on nickel electrode performances [15]. The experiments were performed by means of a Wenking HP72 potentiostat, a PV2 programmer and an Endim 620.02 X–Y recorder.

The charge–discharge curves were performed in a half-cell consisting of the sintered nickel electrode (70 × 35 × 1 mm) as working electrode, a SCE as reference and a nickel plate as counter electrode. All experiments were conducted at room temperature.

The different forms of active material (uncycled, charged and discharged) were characterized by X-ray diffraction (XRD) and scanning electron microscopy (SEM).

X-ray diffractograms were obtained with a DRON 3 powder diffractometer, using CuK$_\alpha$ radiation. SEM photographs were taken using a BS 340/1990 Tesla-Brno microscope.

Table 3
Oxygen evolution overpotentials and hydrogen evolution overpotentials, in 6N KOH + 35 g/l LiOH electrolyte

Electrode	ε_{O_2} (V)	ε_{H_2} (V)	η_{O_2} (V)	η_{H_2} (V)
Ni	0.420	− 1.280	0.263	0.202
Ni + Co	0.430	− 1.280	0.273	0.202
Ni + Cd	0.440	− 1.290	0.283	0.212
Ni + Co + Cd	0.470	− 1.290	0.313	0.212

Table 4
Coulombic efficiencies of sintered nickel electrode

Electrode	Q_{charge}(mAh)	$Q_{discharge}$ (mAh)	r_F (%)	ε_r (V)
Ni	550	383	69.64	0.274
Ni + Co	550	475	86.36	0.242
Ni + Cd	550	433	78.73	0.280
Ni + Co + Cd	550	450	81.81	0.285

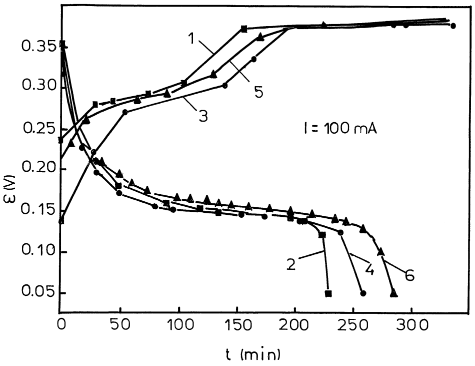

Fig. 3. Charge–discharge curves of Ni (1–2), Ni + Cd (3–4), and Ni + Co (5–6) electrodes, at $I = 100$ mA, in 6N KOH + 35 g/l LiOH.

3. Results and discussion

The processes that occur on sintered nickel electrode were evidenced by cyclic voltammetry [15]. The voltammograms of nickel electrodes without additives in active material, at four sweep rates are shown in Fig. 1.

The potential was scanned between cathodic value at which hydrogen evolution reaction (HER) occurs and anodic value at which oxygen evolution reaction (OER) occurs. The anodic peak was associated with the oxidation of Ni(OH)$_2$ to NiOOH (charge process) and the cathodic peak with the reduction of NiOOH to Ni(OH)$_2$ (discharge process).

The stabilized form of the voltammograms at $v = 20$ mV/s was attained in the second cycle (curve 2) after the addition of 35 g/l LiOH in the 6N KOH electrolyte. It is evident, from the anodic and cathodic peaks positions, that a lower sweep rate is beneficial for the reversibility of the processes.

The voltammograms of sintered nickel electrodes containing cobalt and cadmium additives in active material, compared with the voltammogram of nickel electrode

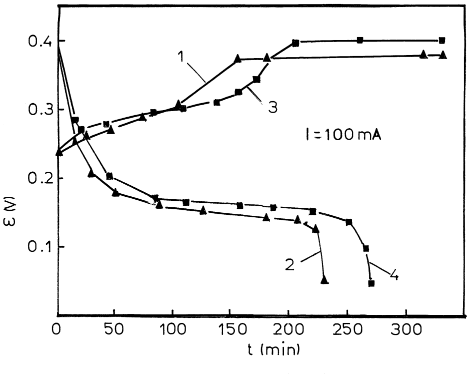

Fig. 4. Charge–discharge curves of Ni (1–2), Ni + Co + Cd (3–4), at $I = 100$ mA, in 6N KOH + 35 g/l LiOH.

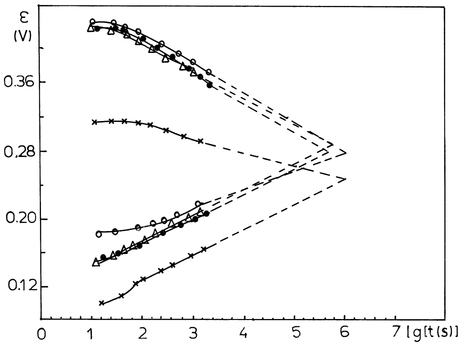

Fig. 5. Evaluation of reversible potentials of Ni (o), Ni + Co (x), Ni + Cd (•), and Ni + Co + Cd (△) electrodes, in 6N KOH + 35 g/l LiOH.

without additives, in 6N KOH + 35 g/l LiOH electrolyte, at $v = 1.11$ mV/s are shown in Fig. 2.

In all these voltammograms were identified only the two peaks corresponding to $Ni(OH)_2$/NiOOH couple redox reactions. The presence of the additives in active material of sintered nickel electrodes has a variety of effects on the cyclic voltammograms: changes of the peaks position, of the average potential, $\varepsilon' = (\varepsilon_{a,p} - \varepsilon_{c,p})/2$, of the difference of peaks potentials, $\Delta\varepsilon_p = \varepsilon_{a,p} - \varepsilon_{c,p}$, and of the ratio of cathodic to anodic peak currents, $I_{c,p}/I_{a,p}$ (Table 2).

Examination of Table 2 data shows the beneficial effect of cobalt and cadmium additives, on the reversibility of the electrode processes, manifested by decrease of $\Delta\varepsilon_p$ and by a slight increase of $I_{c,p}:I_{a,p}$ ratio.

The average potential was shifted to more cathodic values for Ni + Co and Ni + Co + Cd, respectively, and to more anodic values for Ni + Cd electrodes.

The estimation of electrocatalytic effects of cobalt and cadmium additives in active material on OER and HER was made by values of oxygen evolution overpotentials, η_{O_2} and hydrogen evolution overpotentials, η_{H_2} (Table 3). The overpotentials were calculated using the experimentally recorded values of OER and HER potentials and the reversible potential values, $\varepsilon_{r,O_2} = 0.157$ V/SCE and $\varepsilon_{r,H_2} = -1.078$ V/SCE, respectively [16].

The cobalt and cadmium compounds determined the increase of η_{O_2} in the order: Co + Cd (0.050 V) > Cd (0.020 V) > Co (0.010V).

Because the increase of η_{O_2} due to cobalt and cadmium additives, the oxygen evolution is minimized, determining a better reversibility of the electrode processes, an improved charge of active material and better coulombic efficiencies, r_F than for electrodes without additives (Table 4).

The values of parameters presented in Table 4 were obtained from the charge–discharge curves recorded in half-cell, in galvanostatic regime ($I = 100$ mA), at room temperature (Figs. 3 and 4).

The decrease of plateaus corresponding to OER (the charge curves of Figs. 3 and 4), at addition of cobalt and

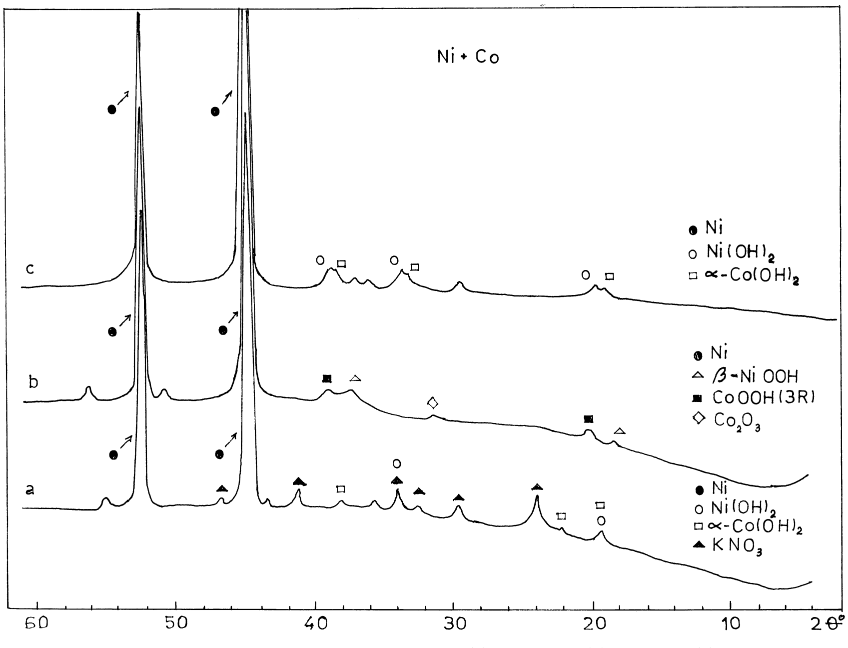

Fig. 6. X-ray diffractograms of Ni + Co electrode: (a) uncycled, (b) charged, (c) discharged.

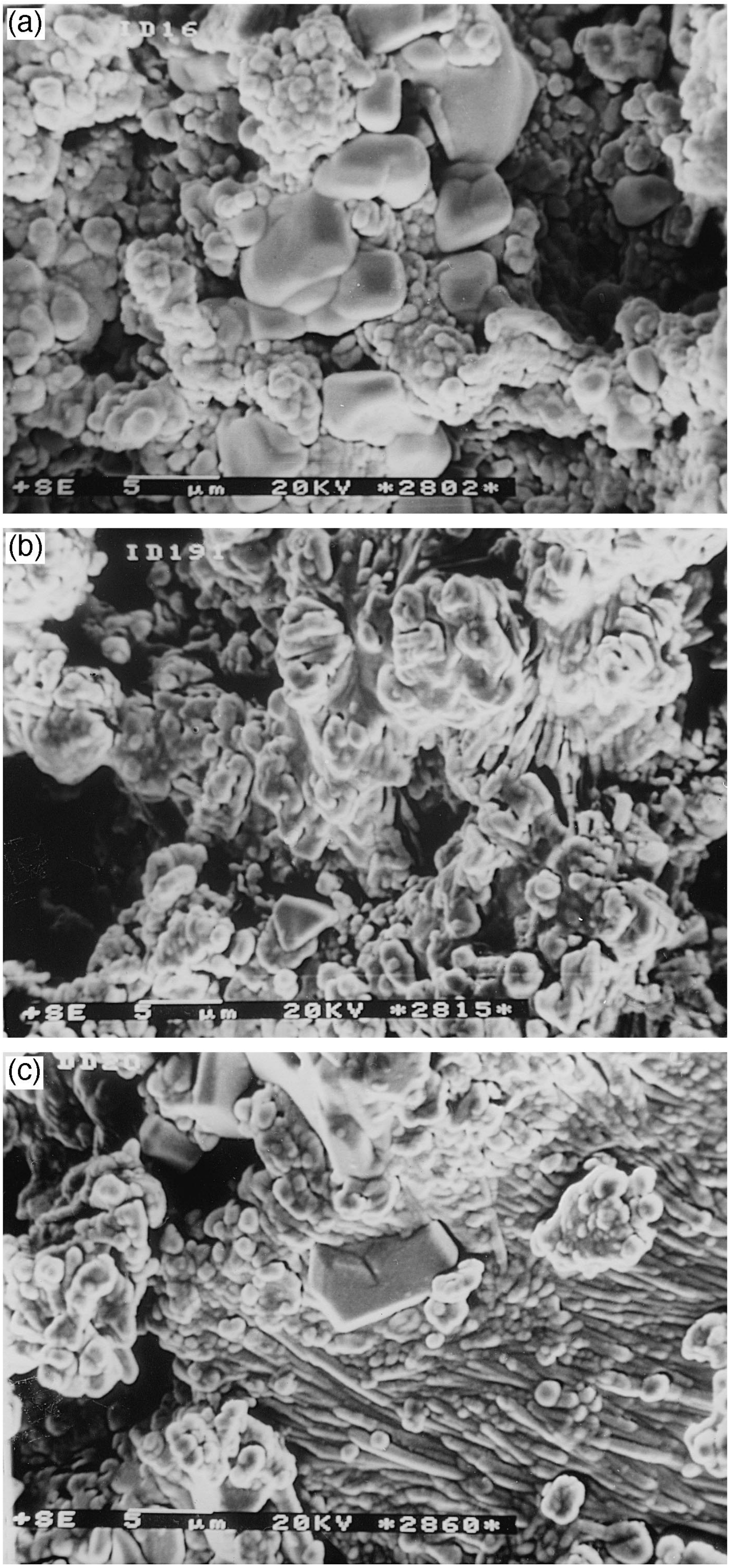

Fig. 7. SEM photographs of Ni + Co electrode: (a) uncycled, (b) charged, (c) discharged.

cadmium, also demonstrates the increase of the charge efficiency and hence, the improvement of the discharge characteristics of Ni + Co, Ni + Cd, and Ni + Co + Cd electrodes.

The reversible potential ε_r of nickel hydroxide electrode, evaluated from the ε vs. *lg t* data by intersecting the anodic and cathodic recovery lines (Fig. 5) was shifted to more cathodic value by $Co(OH)_2$ and to more anodic value by $Cd(OH)_2$ (Table 4). The ascending recovery lines were obtained after a discharge of the electrodes with $I = 100$ mA, to 0.05 V. The descending recovery lines were obtained after a charge of the electrodes with $I = 100$ mA for 5.5 h.

Because the shift of ε_r to more cathodic value by addition of $Co(OH)_2$, the charge takes place at less positive potentials (Fig. 3, curve 5, at values of the potential above 0.3 V) and it is more complete, minimizing the OER. On the other hand, it is considered that $Co(OH)_2$ improves the reversibility of the electrode processes due to the electrocatalytic effect of $CoOOH/Co(OH)_2$ redox couple [17–19]. This effect is probably related to a particular structure resulted by the insertion of cobalt ions in the nickel hydroxide lattice.

Our previous structural investigations of the nickel electrode without additives, by XRD and SEM, demonstrated the presence of α and β-$Ni(OH)_2$ in the discharged electrode and of γ and β-NiOOH in the charged electrode [15].

The structural investigations of Ni + Co electrode demonstrated the existence of CoOOH in the charged electrode and α-$Co(OH)_2$ in the discharged electrode (Fig. 6).

SEM investigation of the uncycled Ni + Co electrode (Fig. 7a) shows besides amorphous $Ni(OH)_2$ active material, microcrystalline aggregates of $Co(OH)_2$. In the charged electrode (Fig. 7b), lamellar crystals of β-NiOOH and small crystals of CoOOH having trigonal symmetry were evidenced. In the discharged electrode (Fig. 7c), lamellar aggregates of $Ni(OH)_2$ and small crystals of α-$Co(OH)_2$ were found.

Although, compared with nickel electrode, ε_r for Ni + Cd electrode is slightly shifted to more anodic value, the charge process is more efficient due to the increase of OER overpotential.

At the same time, the cadmium compounds have a favourable effect on the reversibility of the electrode processes. The XRD structural investigations confirmed the presence of CdO in the charged electrode and $Cd(OH)_2$ in the discharged electrode (Fig. 8).

Cadmium did not change the oxidation state, because in the conditions in which the electrode was cycled, the potential values corresponding to $Cd(OH)_2 \rightarrow Cd$ transformation were not attained.

SEM investigations of uncycled Ni + Cd electrode (Fig. 9a) shows the presence of small crystals of $Cd(OH)_2$ in the gaps between the $Ni(OH)_2$ tabular crystals. In the microcrystalline structure of charged electrode (Fig. 9b), prismatic crystals of CdO were identified. In the discharged

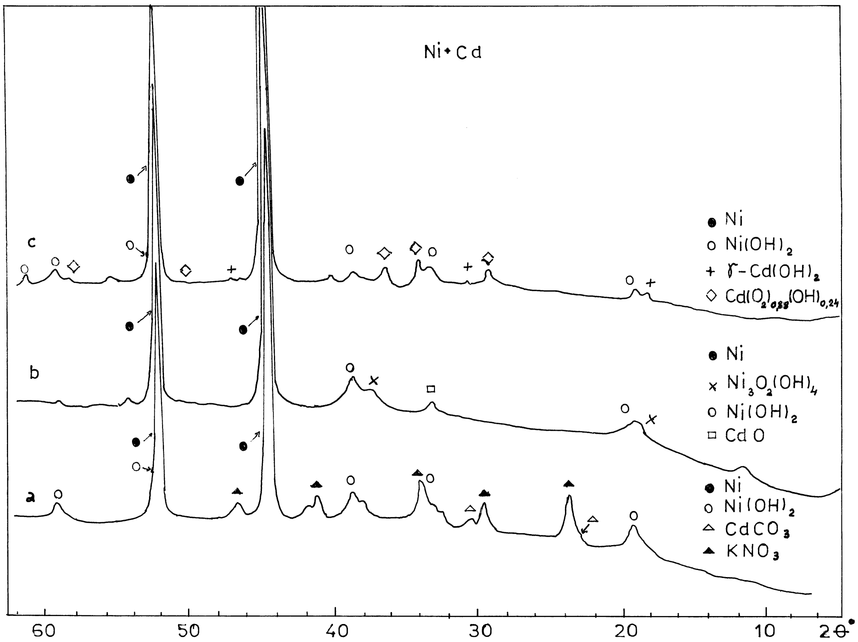

Fig. 8. X-ray diffractograms of Ni + Cd electrode: (a) uncycled, (b) charged, (c) discharged.

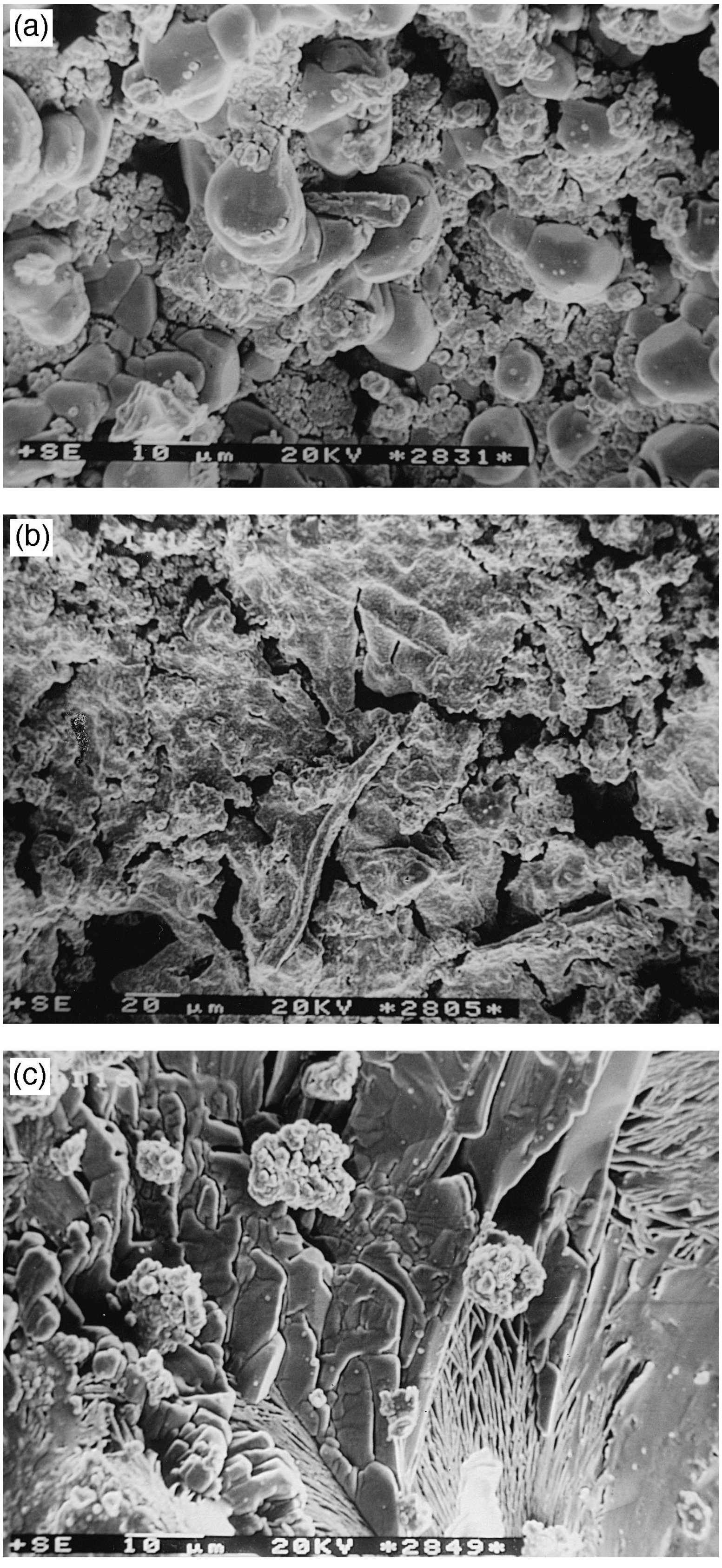

Fig. 9. SEM photographs of Ni + Cd electrode: (a) uncycled, (b) charged, (c) discharged.

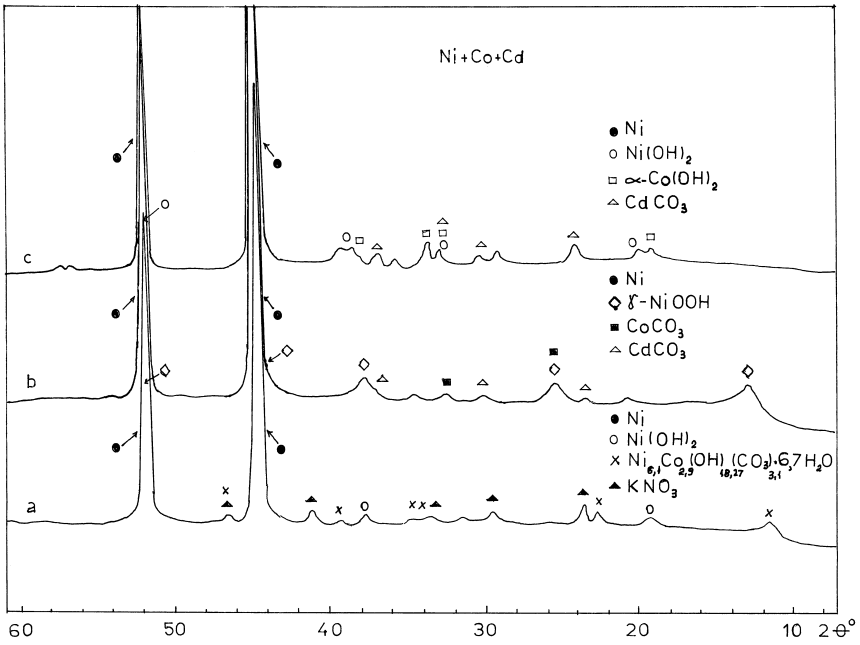

Fig. 10. X-ray diffractograms of Ni + Co + Cd electrode: (a) uncycled, (b) charged, (c) discharged.

electrode (Fig. 9c) on the acicular–lamellar crystals of $Ni(OH)_2$, there are γ-$Cd(OH)_2$ crystals in the efflorescences form.

The Ni + Co + Cd electrode presents better discharge capacity and coulombic efficiency than nickel electrode without additive (Table 4). The XRD investigations demonstrated that the active material of Ni + Co + Cd electrode in charged state is γ-NiOOH (Fig. 10), which, according to literature data, confers to electrode a more reduced self-discharge than β-NiOOH [20].

SEM photographs of uncycled Ni + Co + Cd (Fig. 11a) indicates the presence of some microcrystals of cobalt and cadmium hydroxides on the amorphous active material surface. In the charged electrode (Fig. 11b), besides charged active material, γ-NiOOH, there are cobalt and cadmium compounds as carbonates. In the discharged electrode (Fig. 11c), cadmium compound remains as rhombohedral $CdCO_3$, while cobalt compound appears as trigonal crystal of α-$Co(OH)_2$.

The presence of $CdCO_3$ in the active material is a result of the action of CO_2 from air on KOH electrolyte solution and of the pronounced tendency of substitution of NO_3^- remained from the preparation step by CO_3^{2-} ions.

The Ni + Co + Cd electrodes can be recommended for Ni–Cd batteries used in electrochemical storage of energy. In addition, the presence of $Cd(OH)_2$ as antipolar mass ensures the protection of sealed Ni–Cd batteries against accidental overdischarges.

4. Conclusions

From the studies performed on sintered nickel electrodes having cobalt and cadmium compounds as additives in active material, the following conclusions can be drown.

(a) The electrochemical characteristics and the performances of electrodes, established by cyclic voltammetry and charge–discharge curves, are in accordance with the structures and the compositions of electrodes, established by X-ray diffraction and scanning electron microscopy.

(b) The cobalt hydroxide addition enhanced the electrode performances by the increase of OER overpotential, the decrease of charge potential and the electrocatalytic effect of $CoOOH/Co(OH)_2$ couple on the electrode processes.

(c) The cadmium hydroxide addition enhanced the electrode performances by the increase of OER overpotential and improvement of electrode processes reversibility.

(d) By XRD and SEM has been demonstrated that the presence of cobalt and cadmium hydroxides determines the appearance of different forms of charged active material: β-NiOOH in Ni + Co electrode, $Ni_3O_2(OH)_4$ in Ni + Cd electrode and γ-NiOOH in Ni + Co + Cd electrode.

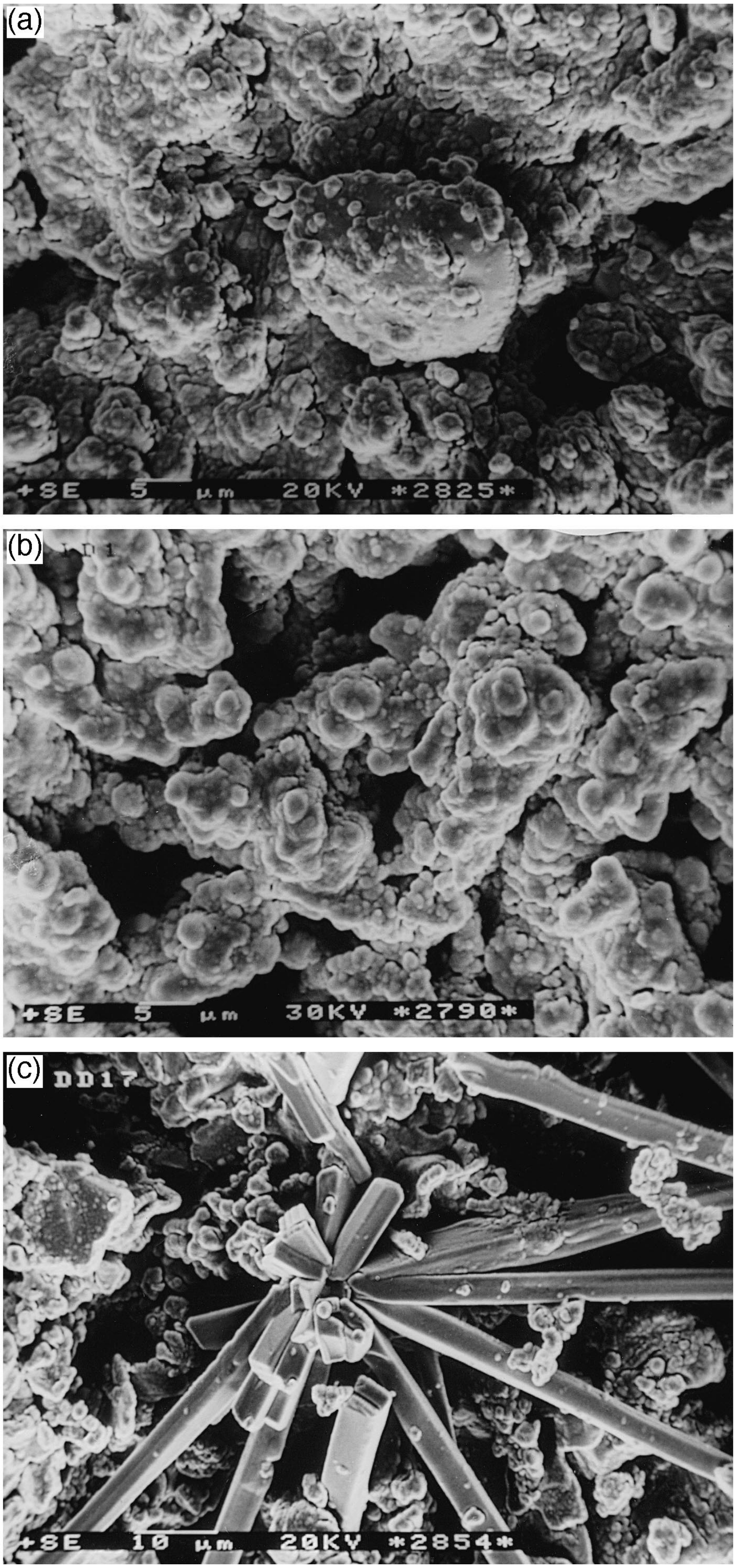

Fig. 11. SEM photographs of Ni + Co + Cd electrode: (a) uncycled, (b) charged, (c) discharged.

(e) From the investigated electrodes, the Ni + Co + Cd electrodes have been selected for Ni–Cd batteries due to their high performances and the protection ensured by $Cd(OH)_2$ presence against accidental overdischarges of the sealed batteries.

References

[1] L. Oniciu, E.M. Rus, in: Dacia (Ed.), Surse Electrochimice de Putere, Cluj-Napoca, 1987.
[2] J. Desilvestro, O. Haas, J. Electrochem. Soc. 137 (1990) 5c.
[3] R. Barnard, C.F. Randell, F.Y. Tye, J. Appl. Electrochem. 10 (1980) 109.
[4] H. Bode, K. Dehmelt, J. Witte, Electrochim. Acta 11 (1966) 1079.
[5] D.A. Corrigan, S.L. Knight, J. Electrochem. Soc. 136 (1989) 613.
[6] G.W.D. Briggs, P.R. Snodin, Electrochim. Acta 27 (1982) 565.
[7] P. Oliva, J. Leonardi, J.F. Laurent, C. Delmas, J.J. Braconnier, M. Figlarz, F. Fievet, A. de Guibert, J. Power Sources 8 (1982) 229.
[8] B.C. Cornilsen, X. Shan, P.L. Loyselle, J. Power Sources 29 (1990) 453.
[9] L. Oniciu, E.M. Rus, P. Ilea, V. Voina, D. Constantin, Rev. Chim. 36 (1985) 340.
[10] M.E. Unates, M.E. Folquer, J.R. Vilche, A.J. Arvia, J. Electrochem. Soc. 139 (1992) 2697.
[11] D.A. Corrigan, R.M. Bendert, J. Electrochem. Soc. 136 (1989) 723.
[12] P.V. Kamath, M.F. Ahmed, J. Appl. Electrochem. 23 (1993) 225.
[13] L. Demourgues-Guerlou, C. Delmas, J. Electrochem. Soc. 141 (1994) 713.
[14] L. Oniciu, D. Constantin, E.M. Rus, V. Voina, C. Corabian, Studia Univ. ‘Babes-Bolyai’, Ser. Chem. 39 (1994) 218.
[15] D.M. Constantin, PhD Thesis, ‘Babes-Bolyai’ Univ., Cluj-Napoca, Romania, 1996.
[16] T.S. Balasubramanian, K. Vijayamohanan, A.K. Shukla, J. Appl. Electrochem. 23 (1993) 947.
[17] S.I. Cordoba, R.E. Carbonio, M. Lopez Teijelo, V.A. Macagno, Electrochim. Acta 31 (1986) 1321.
[18] C.A. Gervasi, J.R. Vilche, P.E. Alvarez, Electrochim. Acta 41 (1996) 455.
[19] S.K. Tiwari, P. Chartier, R.N. Singh, J. Electrochem. Soc. 142 (1995) 148.
[20] B.B. Ezhov, O.G. Malandin, J. Electrochem. Soc. 138 (1991) 885.